Role of conformational disorder in the electronic structure of conjugated polymers: Substituted polydiacetylenes

Vladimir Dobrosavljević* and Richard M. Stratt
Department of Chemistry, Brown University, Providence, Rhode Island 02912
(Received 12 May 1986)

We consider a novel type of disorder relevant to the electronic structure of certain conjugated polymers: disorder induced by *conformational* changes in the chain geometry. A prototypical system in which strong disorder of this variety can be present is a substituted polydiacetylene. Both in the solid phase and in solution, these polymers undergo conformational transitions accompanied by color changes as one raises the temperature. We first present a simplified model for this transition which defines a probability distribution for conformational disorder. Real-space renormalization-group methods are then used to calculate the density of states and localization length for the model. Our results indicate that conformational disorder can cause qualitative changes in electronic structure in a fashion consistent with experiments. We also conclude that since such disorder is correlated, more than one length scale is needed to characterize an electronic state. In particular, "conjugation length" does not suffice.

I. INTRODUCTION

The electronic structure of conjugated polymers continues to be of interest, not least because of the possibility afforded for strong coupling to changes in the geometry of polymer chain backbones. However, it is the low effective dimensionality of such polymers that makes this coupling most efficient in producing unusual phenomena. In one dimension, the coupling of the electronic structure to *longitudinal* distortions can lead to a Peierls transition,[1] which opens a gap in the electronic density of states at the Fermi surface. As a consequence, updoped conjugated polymers behave as semiconductors with optical gaps of the order of few electron volts. Moreover, on doping, compounds such as polyacetylene and polyparaphenylene support new types of elementary excitations such as solitons[2] and bipolarons.[3]

In other classes of conjugated polymers, in particular, substituted polydiacetylenes,[4] the coupling of the electronic structure to *conformational* changes in chain geometry is especially important. Specifically, energy scales for rotations around the carbon-carbon single bonds (Fig. 1) are comparable to thermal energies, so that one expects a considerable number of such rotations to be present, even at room temperature. Since the value of the overlap integral corresponding to a particular single bond goes as a cosine of the angle of rotation, the electronic structure is considerably perturbed by this type of conformational change and is therefore likely to be correspondingly sensitive to variations in the condensed phase environment.[5]

Polydiacetylenes themselves have been the subject of quite a number of experimental studies.[6–19] The methods used have spanned the gamut of solid- and liquid-state probes, including ultraviolet and visible absorption,[6,8,9,11–13] light scattering,[13–15] resonance Raman spectroscopy,[6–8,10,11] x-ray crystallography,[18] and NMR studies.[11,15,19] What motivated most of these investigations was the observation that an abrupt color change occurs as one varies the temperature, both when polydiacetylene is crystalline[6,7] and when it is in solution.[10] A similar color change is observed in solution when the fraction of the polar solvent is varied.[12] Inasmuch as the solution behavior is largely independent of the polymer concentration (over several orders of magnitude)[12] and since the same phenomenon seems to be characteristic of the solid, the color change itself may be viewed as largely a single-chain phenomenon (though aggregation of chains

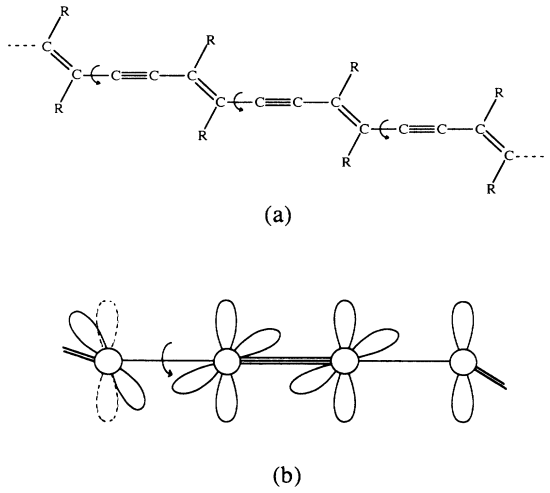

FIG. 1. (a) Structure of a substituted polydiacetylene. The letter *R* represents side chains and the arrows represent the low energy rotations around single bonds capable of creating disorder in the electronic structure. (b) An enlargement of single-bond—triple-bond—single-bond region of the polymer showing how the relative orientations of the *p* orbitals change when a rotation is performed.

 ©1987 The American Physical Society

probably does occur[20]). The one-chain picture gets additional support from recent birefringence studies.[16] These and light scattering experiments in solution[13–15] demonstrate that the color change is associated with a considerable change in the radius of gyration, suggesting in turn that the color change is caused by some conformational transformation, such as a rod-to-coil transition. Infrared studies on polydiacetylenes with hydrogen-bonding side chains have been able to show that the number of broken hydrogen bonds increases as the transition is crossed, confirming the presence of conformational defects in the chain.[12,17]

More generally, detailed optical-absorption measurements[6,8,9,11–13] indicate that the color change is caused by a shift of the absorption edge to higher energies as the temperature or the fraction of polar solvent is increased. How this shift happens is not clear, but resonance Raman experiments[6–8,10,11] imply that the disordered form of the polymer is associated with different electronic absorptions, which seem to be affiliated with higher double- and triple-bond stretching frequencies than are present in the ordered form. More recent experiments[10] have even disclosed hysteresis phenomena, which suggests that the conformational structures leading to the new absorptions have extremely long relaxation times.

We should note that, historically, the first attempts to understand the observed color change did not consider a conformational origin to the transition.[7] Instead they focused on the changes in dimerization—the pattern of alternating single and multiple bonds. The idea was that the chain could make transitions from the ene-yne (double-single-triple-single) structure pictured to a butatriene (three consecutive double-bond) structure. However, both x-ray[18] and NMR[11,15,19] experiments and theoretical considerations[21] demonstrated that only the ene-yne structure is present to a significant extent. Hence the longitudinal distortions that give rise to changes in dimerization cannot be playing an important role here. Of course, in polyacetylene, it was precisely these distortions that proved vital for understanding the possibility of soliton excitations.[2]

To try to understand the somewhat different effects of conformational changes, consider a simplified picture where only rotations of $\pm\pi/2$ are allowed.[22] These rotations totally break the conjugation, separating the polymer chain into electronically independent "submolecules." Experimental studies on finite-length conjugated chains have shown that the effects of having a finite conjugation length is to increase the values both of the optical gap and the appropriate vibrational frequencies.[6] The same conclusions can be obtained from simple theoretical considerations of finite-length chains.[23] Alternatively, as shown in Sec. II, another type of conformational change, uniform rotations by the same angle on each monomer (leading to a "wormlike chain" in the language of Ref. 11) produces similar effects.[24] From either point of view, we can conclude that the existence of conformational defects is consistent with a general shift in optical and vibrational frequencies to higher values.

These pictures thus suggest a scenario in which the color change is induced by the chain undergoing a rod-to-coil transition. The preponderence of conformational defects in the coiled form would certainly account for the dramatic change in the character of the electronic structure that one sees in changing the temperature or the solvent. Within this framework, the immediate question becomes one of what the driving force for the rod-to-coil transition is, a question on which there is no unanimity, though several authors[22,25–28] have considered possible physical mechanisms.

Quite generally, the entropic effects associated with both backbone and side-chain motion tend to favor the disordered (coiled) state. However, to account for the relatively sharp transition (or even, possibly, a true phase transition) some *cooperative* mechanism stabilizing the extended (rodlike) state is needed. Stratt and Smithline[22] considered cooperativity induced by the energetics of a conjugated π system. Such a model, though, cannot account for the existence of a sharp transition. Berlinsky *et al.*[25] used a phenomenological statistical mechanical model inspired by the classical Zimm-Bragg description of the helix-coil transition.[26] The microscopic origin of the needed cooperativity here was the presence of the "loop entropy"[26] such as is found in DNA, although it remains unclear as to precisely how these ideas might apply to polydiacetylene. Goldenfeld and Halley[27] even proposed an entirely new mechanism for general rod-to-coil transitions in polymers based on vibrational entropy. Still another picture, more specific to conjugated polymers, was put forward by Schweizer,[28] who invoked the higher polarizability of extended sections of the conjugated polymer chains as a driving force for the transition. In a careful study he was able to show that polarizability considerations can lead to a genuine phase transition for some values of his parameters. There are yet other notions as to the mechanism, but perhaps at this stage it would be best to note that a final consensus has not been reached. Nevertheless, the fact that there is a conformational transition from an ordered to a disordered state seems almost certain.

What is clearly the next step, then, is to focus on how the electronic structure itself is realistically affected by changes in conformation. None of the work we have been discussing explicitly considered rotations other than $\pm\pi/2$, except Ref. 11. Moreover, in what has been done to date, drastic simplifications have been made to make the electronic structure problem exactly solvable, missing in the process a great deal of interesting physics: what we will call the effects of the *conformationally induced disorder*. Accordingly, the main theme of this paper will be to examine the consequences of this disorder (and *not* the specific mechanism that causes it). One can appreciate the particular importance of disorder in polydiacetylene by noting that conformational motion is very slow on the time scale for electronic motion. Therefore, the disorder introduced by such a motion can be considered to be static or quenched when the electronic structure is examined—and quenched disorder is what makes it possible to have the quantum coherence necessary for Anderson localization and all the nontrivial effects associated with it.[29]

The special significance of disorder has been evident ever since Anderson's pioneering work in 1958.[30] In par-

ticular, it is known that the simple presence of disorder can have profound effects on the nature of the electronic wave functions: Localization can occur. In the last several years the interest in disordered systems in general has significantly increased with the development of new ideas and powerful methods, such as the scaling theory[31] and the renormalization-group techniques.[32] It is now well established that all states are localized in one and two dimensions, whereas in three-dimensional systems some states can remain extended. In one dimension, the effects of disorder are sufficiently strong that disorder can have nontrivial effects not only on the nature of the electronic wave functions, but also on the structure of the density of states.[33] (It is also interesting to mention that, in one dimension, the density of states itself contains information on localization,[34] unlike the situation in higher dimensions where the density of states is smooth and is not as dramatically influenced by disorder.) In the presence of disorder, the density of states can develop complicated, highly structured forms, which, in some energy intervals, can even have a fractal (self-similar) nature.[33] Such complicated behavior of the density of states is difficult, if not impossible, to describe in the framework of any perturbation or effective medium (mean-field) theory. However, renormalization-group methods which include coherent scatterings on all length scales have been recently devised.[32] These methods, although approximate, have been able to reproduce much of the complicated structure in the density of states and to calculate the corresponding localization lengths in good agreement with numerical results. Consequently, we will be able to make use of such calculational schemes in investigating the details of the electronic structure of even as strongly disordered a quasi-one-dimensional system as polydiacetylene.

To summarize the scope of this paper, then, in Sec. II we perform model calculations for the energetics of different conformational defects. Using these calculations as a guide, a simplistic model for the conformational transition is then presented in order to define a detailed probability distribution for disorder. The statistical mechanics of this model can be solved exactly. In Sec. III we define the framework in which we calculate the electronic structure and we study the effects of the disorder using renormalization-group methods. The density of states and corresponding localization lengths are calculated and the results presented for different amounts of disorder. Finally, Sec. IV discusses our results and points out some implications of our work. Limitations of our treatment are also discussed, as well as possible future extensions.

II. A MODEL FOR CONFORMATIONAL DISORDER

A. The energetics of conformational defects

Before specifying a model for our rod-to-coil transition, we first take up the question of what types of conformational defects are present in the disordered (coiled) phase. As we have noted, most of the authors have considered only $\pi/2$ rotations,[22,28,35] whereas Wenz, Müller, Schmidt, and Wegner[11] have suggested "wormlike" chains with continuous twists by a small angle on each monomer. We can get an idea of the energy scales of these different defect types, and of the forms of the corresponding rotational potentials, by performing model calculations on long chains with specified geometries. Consider, as a starting point, a simple tight-binding model with the backbone p orbitals taken as a basis and the bond lengths kept fixed at their planar values. It is worth mentioning that, even at this level, polydiacetylene, unlike polyacetylene, has p_y orbitals perpendicular to the plane of the p_x orbitals which create the conjugation [Fig. 1(b)]—a fact which turns out to be energetically very important.

One cannot expect the numerical values obtained in this fashion to be quantitatively accurate. Still, the qualitative features of the results and relative energy costs for different defect types are probably correctly predicted. Numerical values for the hopping elements have been estimated from x-ray data[18] for bond lengths by using the empirical formula[36]

$$V(r)=67.28\exp[-r/(0.424\ \text{Å})]\ \text{eV}\ ,$$

with V the hopping element and r the bond length. The values obtained for single, double, and triple bonds, respectively, are $V_1=2.20$ eV, $V_2=2.66$ eV, $V_3=4.06$ eV. The resulting band structure and density of states for the perfect polydiacetylene (PDA) chain are presented in Fig. 2 with the energy measured from the middle of the optical gap separating the occupied from empty states. The value obtained for this optical-gap energy is 2.12 eV, in reasonable agreement with experiments.[6,8,9,11–13] We also note the isolated δ function peaks at $E=\pm V_3$, corresponding to the off-plane p_y orbitals which are not conjugated in the perfect chain.

With this result defining our reference, we can consider the energy cost of a single rotation performed around a particular single bond (Fig. 1). (The detailed dependence of the transfer integrals on rotational angles is given in Sec. III B.) It has been suggested[35] that $\pi/2$ rotations should have a low energy cost, since although a p_x-p_x

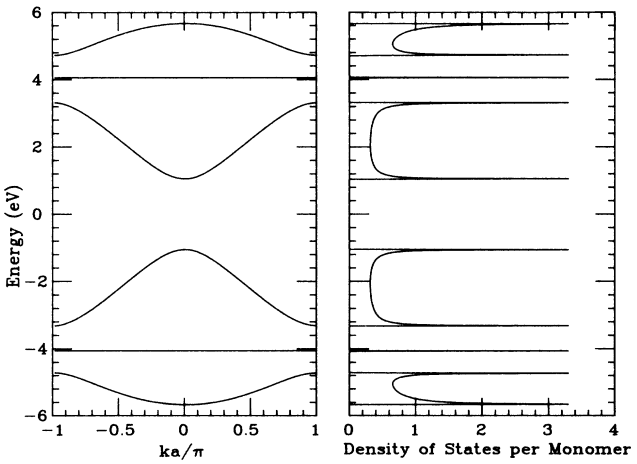

FIG. 2. Band structure and density of states for a perfect polydiacetylene chain. The wave vector k is expressed in units of π/a, where a is the monomer length. The peaks in the density of states are, in fact, Van Hove singularities which we have truncated for clarity. Note that the delta-function peaks at ± 4.06 eV correspond to the out-of-plane (unconjugated) p_y orbitals.

bond is broken, another p_x-p_y bond is formed. Naively, one would then expect that this should be a local minimum of the rotational potential. Our results for the rotational potential presented in Fig. 3, show, however, that $\pi/2$ is actually the energy maximum and that the minima are at 0 and π. The energy cost nonetheless is small, as expected: $E(\pi/2)-E(0)\cong 0.07$ eV.[37] (This figure is probably an overestimate for the energy; the real energy is expected to be very small, in agreement with Ref. 35.) We are forced to conclude that $\pi/2$ defects are, in fact, the most unlikely ones, so that pictures which include only such defects are unrealistic for purposes other than estimating general trends in the electronic behavior. Still, the basic physics is captured by any model which permits low-energy conformational defects. Rotations around single bonds do not explicitly break any *local* bonds and therefore cost very little energy. What they do accomplish is an *interruption of conjugation* along the chain backbone. It is precisely this fact that makes it possible to have strong thermally induced disorder at room temperature.

The next question, presumably, is whether these conformational defects are significantly correlated. In order to analyze this, we calculated the interaction energy for two defects (defined to be rotations by an angle ϕ on single bonds) which were separated by N monomers. This interaction turns out to be attractive, but regardless of the value of ϕ chosen, it was always very weak [$V(N=0)\cong -2\times 10^{-3}$ eV] and exponentially dependent on the separation, N. Certainly to within the accuracy we will need in this paper, such interactions can be neglected. Thus, given our result that the energy scales for single bond rotations are of the order, or even possibly smaller, than the thermal energies at room temperature, we expect there to be a more-or-less random distribution of rotational defects in the coiled phase.

B. Defining the model

As we have stressed in the Introduction, the main thrust of this paper is to consider the effects of disorder, *not* the specific origin of the rod-to-coil transition. We do present a simple model for the conformational transition, but we do so because a definite model is necessary in order to define a precise form for the probability distribution of disorder as a function of temperature. Our general conclusions are largely independent of the model.

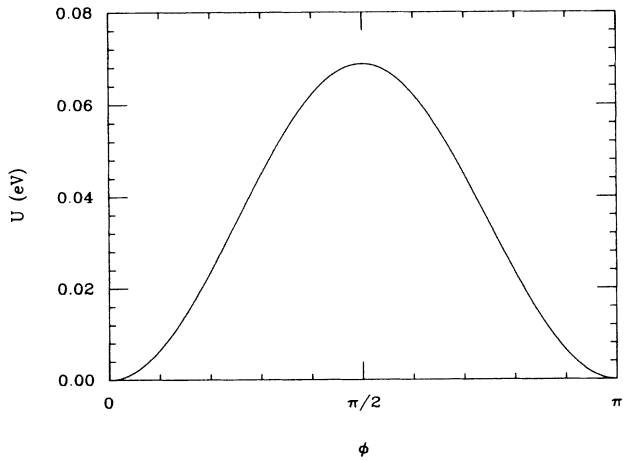

FIG. 3. Effective rotational potential $U(\phi)$ for an isolated rotation by an angle ϕ about a single bond.

This model itself focuses on the role of hydrogen-bonded side chains as a driving force for the transition. To perform rotations around some single bond, the appropriate hydrogen bonds have to be broken at cost of some energy E_b. However, it is necessary to break *two consecutive* hydrogen bonds to set the corresponding side chain free to move (Fig. 4). Since these side chains can be quite long and flexible [in compounds such as poly-3BCMU and -4BCMU (Ref. 12)], allowing them to move liberates a large amount of entropy $S_{\rm ch}$. The hydrogen-bond-breaking dynamics can then be mapped into a one-dimensional lattice gas model with E_b playing a role of the chemical potential and $S_{\rm ch}T$ the role of the coupling parameter. The effective Hamiltonian (or free-energy functional) is

$$H=\sum_i [-(S_{\rm ch}T)\mu_i\mu_{i+1}+E_b\mu_i] , \tag{2.1}$$

where T is the temperature and $\mu_i=0$, 1 is the variable associated with the hydrogen bond being unbroken or broken, respectively. For simplicity, we assume the H bonds break simultaneously on both sides of the backbone. It is easy to see that this assumption does not change our conclusions in any important way. Once the appropriate hydrogen bonds are broken, we will assume that there is free rotation around single bonds. This idealization allows us to immediately write down the probability distribution for having different conformations of the chain:

$$P[\{\phi_i\},\{\mu_i\}]=Z^{-1}\prod_i \exp\{[(S_{\rm ch}/k)\mu_i\mu_{i+1} -(E_b/kT)\mu_i]\} \times[(1-\mu_i)+\alpha\mu_i\delta(\phi_i)] , \tag{2.2}$$

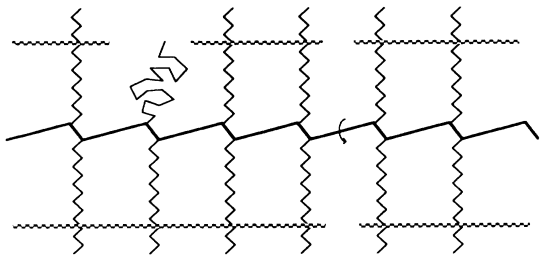

FIG. 4. Hydrogen-bond breaking dynamics. The heavy line represents the polymer backbone and the jagged lines parallel to the backbone represent the hydrogen bonds connecting the side chains. For a rotation to be performed (arrow), hydrogen bonds on both sides have to be broken. However, only when two consecutive hydrogen bonds are broken is a side chain released from the requirement of coplanarity (and the conformational entropy associated with the side chain made available to the system).

where

$$Z \equiv \sum_{\{\mu_i\}} \prod_i \int_0^{\pi/2} d\phi_i \, P[\{\phi_i\},\{\mu_i\}] \tag{2.3}$$

and $\{\phi_i\}$ are the rotational (dihedral) angles on single bonds. The parameter α measures the relative statistical weight of configurations with and without the appropriate hydrogen bonds being broken (with and without single bond rotations). Different choices of α, though, are equivalent to shifting the effective value of E_b after the integration over angles is performed. Since $S_{\rm ch}$ and E_b are empirical parameters which we can fit to the required values, we can choose for convenience $\alpha=\pi/2$. This choice gives

$$\begin{aligned}\tilde{P}[\{\mu_i\}] &\equiv \prod_i \int_0^{\pi/2} d\phi_i \, P[\{\phi_i\},\{\mu_i\}] \\ &= \tilde{Z}^{-1} \exp\left[\sum_i [(S_{\rm ch}/k)\mu_i\mu_{i+1} - (E_b/kT)\mu_i]\right]\end{aligned} \tag{2.4}$$

with

$$\tilde{Z} \equiv \sum_{\{\mu_i\}} \tilde{P}[\{\mu_i\}] \, . \tag{2.5}$$

In other words, this choice of α leaves E_b unchanged after the integration is performed. Note that the average in ϕ is performed only from 0 to $\pi/2$ since the electronic structure depends only on $|\cos\phi|$.

This model is actually isomorphic to a one-dimensional Ising model obtained by setting $\mu=\frac{1}{2}(s+1)$ with $s=\pm 1$. In this language the coupling parameter is $J=-\frac{1}{4}S_{\rm ch}T$ and the effective field is $h=(E_b-S_{\rm ch}T)/4$. It is well known that one-dimensional statistical mechanical models with short-ranged interactions cannot have a true phase transition.[33,38] However, at $T_c=E_b/S_{\rm ch}$ the effective field changes sign, causing a reasonably abrupt transformation (for large J) from the state with $\langle\mu\rangle\simeq 0$ (rodlike) to the state $\langle\mu\rangle\simeq 1$ (coiled). The width of the coexistence region is inversely proportional to J, i.e., to $S_{\rm ch}$. In fact in the limit $S_{\rm ch}\to\infty$, one obtains a first-order phase transition. Therefore, in the framework of this model, it is the entropy gain on allowing the side chains to be free to move that introduces cooperativity and makes possible a relatively sharp phase transformation. The statistical mechanics of this model can, of course, be solved exactly, so we can calculate the fraction of broken bonds as a function of temperature.

Another quantity that will be of interest later is the average length of clusters of unbroken bonds (rodlike segments of the chain), $\langle l\rangle$. At the transition temperature, this length is of the order of the correlation length (where, in the equivalent Ising model language, the effective field is zero), but elsewhere it has to be independently calculated as follows: The probability of having a cluster of exactly n consecutive unbroken bonds is

$$P_n = \langle \mu_i(1-\mu_{i+1})\cdots(1-\mu_{i+n})\mu_{i+n+1}\rangle$$

and the probability that a given unbroken bond belongs to such a cluster is $\tilde{P}_n = nP_n$. As any unbroken bond must belong to some cluster we have

$$\sum_{n=1}^{+\infty} \tilde{P}_n = \langle 1-\mu\rangle$$

and

$$\langle\mu\rangle + \langle 1-\mu\rangle = 1 \, ,$$

where $\langle\mu\rangle$ is the fraction of broken and $\langle 1-\mu\rangle$ of unbroken bonds. Thus the probabilities $\tilde{P}_n$ are correctly normalized (rather than the P_n) and we can define the average cluster length as

$$\langle l\rangle = \sum_{n=1}^{\infty} n\tilde{P}_n = \sum_{n=1}^{\infty} n^2 P_n \, . \tag{2.6}$$

To calculate the probabilities P_n we note that

$$P_n = \Gamma_{n+2} - 2\Gamma_{n+1} + \Gamma_n \, ,$$

where

$$\Gamma_n \equiv \langle (1-\mu_{i+1})\cdots(1-\mu_{i+n})\rangle \, ,$$

and that the fraction of broken bonds is $\langle\mu\rangle = 1-\Gamma_1$. The quantities Γ_n can be readily calculated using standard transfer-matrix techniques,[38] giving the results

$$\begin{aligned}&\langle 1-\mu\rangle = (\lambda_{\rm max}-x)[y^2+(\lambda_{\rm max}-x)^2]^{-1/2} \, , \\ &\langle l\rangle = \langle 1-\mu\rangle(\lambda_{\rm max}+1)/(\lambda_{\rm max}-1)\end{aligned} \tag{2.7}$$

with

$$\lambda_{\rm max} \equiv \tfrac{1}{2}\{(1+x)+[(1-x)^2+4y^2]^{1/2}\} \tag{2.8}$$

and

$$\begin{aligned}&x \equiv \exp[(S_{\rm ch}/k)-(E_b/kT)] \, , \\ &y \equiv \exp[-E_b/2kT] \, .\end{aligned} \tag{2.9}$$

The results from these calculations are plotted in Fig. 5 for different values of $S_{\rm ch}$ (effectively for different side-chain lengths).

Before proceeding to the next section and detailed calculations of the resulting electronic structure, it is worth noting the high- and low-temperature limiting predictions of this model. At low temperatures, where most of the hydrogen bonds are unbroken, rotations are forbidden, so the electronic structure and the size of the gap are approximately equal to those of the perfect chain. Well above the transition, however, most of the hydrogen bonds are broken and the chain undergoes random rotations about single bonds. In this limit, the simplest approximation to the electronic structure possible (the so-called virtual-crystal approximation[33,39]) would come from replacing the random values for the hopping integrals, $V_1(\phi)=V_1\cos\phi$, by their average value:

$$\overline{V_1\cos\phi} = V_1(2/\pi)\int_0^{\pi/2}\cos\phi\, d\phi = (2/\pi)V_1 \, .$$

This approximation is equivalent to postulating a chain with a periodic rotation of $\phi_{\rm eff}=\arccos(2/\pi)$ on every monomer. [Note that $\phi_{\rm eff}\neq\bar{\phi}=\pi/4$ since $\cos(\bar{\phi})\neq\overline{\cos\phi}$.] We see that the "wormlike chain" of Ref. 11 represents, in this sense, a zeroth-order approximation to a more realistic, disordered system because all fluctuations in the distribution of rotations have been neglected.

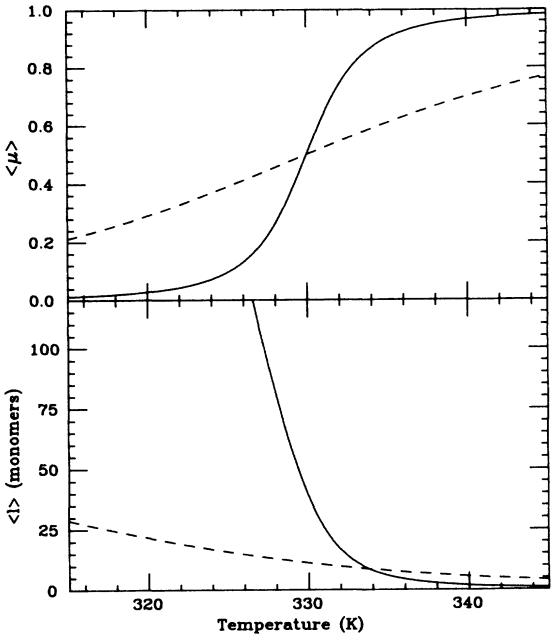

FIG. 5. Conformational statistical mechanics of substituted polydiacetylenes. The top graph shows the fraction of broken hydrogen bonds, $\langle \mu \rangle$, and the bottom graph the average length, $\langle l \rangle$, of rodlike segments of the polymer, both vs temperature. In both graphs the solid curve is calculated for a side-chain entropy of $S_{ch}/k = 6.6 (\simeq 2 \ln 3^3)$, corresponding to two side chains, each with three dihedral angles restricted to being in one of three rotational isomeric states. The dashed curves are for $S_{ch}/k = 4$, corresponding to weaker short-range order. The value of the hydrogen bond energy, E_b, is chosen so that the transition temperature is $T_c = 330$ K.

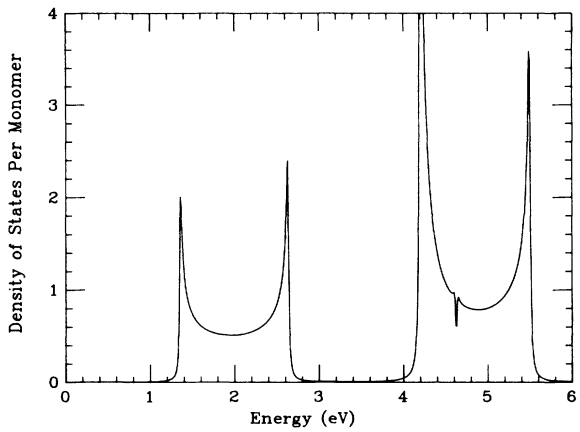

FIG. 6. Density of states in the virtual crystal approximation, assuming random rotations on all monomers ($T \gg T_c$). The lowest energy band remains largely unchanged from its appearance in the perfect chain, although its bandwidth is reduced (see Fig. 2). The two higher energy bands are mixed, however. The plot was done at finite energy resolution [$\eta = 0.01$ eV in Eq. (3.17)] in order to facilitate comparison with later calculations. For $\eta = 0$, the dip at 4.6 eV becomes a genuine gap. In this and subsequent figures we show only the results for positive energies since the density of states is symmetric with respect to $E = 0$.

The electronic structure in this approximate limit is trivially solved, since we again have a periodic system. The resulting density of states, Fig. 6, shows that the absorption edge is indeed shifted to higher energy at high temperatures—in accord with experimental results.[6] The gap has been increased due to a narrowing of the bands as the hopping is reduced. One can also see the mixing of the two higher energy bands as the off-plane p_y orbitals couple to the conjugated p_x system. However, the *structure* of the lower-energy band involved in optical processes remains unchanged since all but the lowest-order effects of disorder have been completely ignored. In the next section we illustrate how a more realistic view of disorder can lead to changes in the band structure as well.

III. ELECTRONIC STRUCTURE IN THE PRESENCE OF DISORDER

A. General considerations

Before embarking on the detailed electronic structure calculations, it is perhaps worthwhile to make a few comments on the nature of disorder as introduced by the conformational motion. Quite generally, since rotations around carbon-carbon single bonds affect the hopping elements, rotations induce off-diagonal disorder. We can be more specific, however. At temperatures well above the transition, where the chain is in the coiled state, an *uncorrelated, continuous* distribution of disorder is present due to the random rotations on every monomer. In the intermediate temperature range, close to the transition, an additional kind of disorder results from the distribution of extended and coiled segments of the chain. Because of the cooperativity of hydrogen-bond breaking (Sec. II), this further *binary disorder* is characterized by a degree of short-range order.

Our general objective, then, is to answer the question of what qualitatively new effects can be caused by the different types of disorder present. In particular, since we are interested in optical and vibrational properties, the first thing we should consider is the change in the structure of the density of states that results from disorder. In order to give a physical interpretation to these new structures we would like to associate characteristic length scales to the corresponding wave functions. Accordingly, we shall also calculate the localization length as a function of energy and discuss how it is related to the spatial extent of the wave functions.

The problem of calculating the electronic structure in the presence of such complicated types of disorder is quite a formidable one, so that a number of rather restrictive simplifications are necessary in order to make the problem accessible to current theoretical methods. In what follows we shall describe these approximations and briefly discuss their individual relevance. We have already mentioned that the conformational motion of the chain is sufficiently slow on the time scale for electronic processes that we can consider the chain as static when evaluating the electronic structure. Because of the bulkiness of side chains and the

finite viscosity of the solvent, it appears that this approximation is realistic. Another simplification will be to ignore both the changes in dimerization (bond length) and the presence of longitudinal phonons, both of which should be relatively unimportant, since the corresponding changes in the chain geometry are much less effective in perturbing the electronic structure than conformational ones.

A more serious limitation, though, is introduced by treating the electronic system in the independent-electron approximation, ignoring the effects of electron-electron correlations. Even with no disorder this formulation can lead to erroneous predictions for the symmetries of excited states and the corresponding transition probabilities, as is well established for small conjugated molecules.[40] However, there are indications that these effects are less pronounced in long conjugated polymers.[41] Experimental optical spectra have, over the years, been relatively successfully interpreted (at least on the qualitative level) using independent-electron models.[6] Moreover, recent studies on doped conjugated polymers such as polyacetylene have shown that the predictions of the existence of solitonlike excitations (for example) are not qualitatively changed when the correlation effects are explicitly included.[42]

The *interplay* between electron-electron correlations and disorder, on the other hand, has recently become a focus of increased interest, in relation to phenomena such as the fractional quantum Hall effect and the electron glass.[43] This interesting subject is still in its infancy, in that the current level of understanding of such effects is nowhere near that of disordered systems with noninteracting electrons. We shall comment on possible implications of the interplay of correlations and disorder in conjugated polymers in the concluding section of this paper; for the time being we limit our attention to the noninteracting electron picture, since the inclusion of correlations clearly deserves to be the object of a separate study. In this framework, we use the simple tight-binding model, a model which has been widely used to investigate the effects of disorder on various systems. Because of its frequent use, a number of theoretical approaches for studying disordered tight-binding models have been developed and tested. Let us now briefly consider the applicability of some of those methods to the study of disordered polydiacetylenes.

The simplest approach, of course, is to do perturbation theory in the strength of disorder.[39] To analyze strongly disordered systems, where perturbation theory fails, various effective medium theories such as the virtual-crystal approximation (VCA), average-T-matrix approximation (ATA), and the coherent-potential approximation (CPA), have been devised.[33,39] Although these methods have met with considerable success in application to higher-dimensional systems, they fail to reproduce the details of complicated densities of states in one dimension. Worse still, these theories are unable to account for the presence of localization.[33,39] Fortunately, new calculational schemes for one-dimensional systems have been developed recently, combining the ideas of effective medium theories and real-space renormalization-group (RG) methods.[32] The new methods give qualitatively different results from effective medium theories. In particular, the Green's functions obtained from these methods have the strongly singular form characteristic of disordered one-dimensional systems. The resulting densities of states and localization lengths also show very good qualitative agreement with numerical results. By virtue of the nature of the technique, renormalized counterparts of all the effective medium theories exist,[32,44] but it has been demonstrated empirically that the best results are obtained using the renormalized average-T-matrix method (RATM).[32] In the rest of this section we shall apply RATM to study the effects of disorder in polydiacetylene.

B. Density of states

The RG methods that we shall use have been developed for simple tight-binding chains with site disorder. In our case, bond disorder is present and the chain has a somewhat more complicated structure, with more than one orbital on some sites. The decimation procedure therefore has to be carried out in a slightly different fashion. For completeness, we shall briefly review the basic ideas of RATM,[32] and describe how it can be applied to polydiacetylene, but the details of the derivation are given in the Appendix.

In the tight-binding model, the electronic Hamiltonian is given by

$$\hat{H}=\sum_{i\neq j} t_{ij}\,|\,i\,\rangle\langle\,j\,|\ , \tag{3.1}$$

where $|\,i\,\rangle$ is the state vector corresponding to the ith orbital, and the t_{ij} are the corresponding hopping elements, which are functions of the chain conformation. The way the orbitals are indexed is shown in Fig. 7(a). Because of the cylindrical symmetry of the triple bond only the *relative* orientation of the p_x orbitals at the ends of each monomer is important, so that we can consider the rotation to be performed on only one single bond in each monomer. Thus, if we allow only nearest-neighbor hoppings, we have: $t_{6n+1,6n+2}=V_1\sin\phi_n$, $t_{6n+1,6n+3}=V_1\cos\phi_n$, $t_{6n+2,6n+5}=t_{6n+3,6n+4}=V_3$, $t_{6n+4,6n+6}=V_1$, $t_{6n,6n+1}=t_{6n+6,6(n+1)+1}=V_2$, for $n=1,2,\ldots$ with $t_{ij}=t_{ji}$ and all other hopping elements equal to zero. Here n is the index of the nth monomer (unit cell), which has six orbitals in it, and ϕ_n is the single-bond rotational angle on the nth monomer.

The basic idea of RG methods is to treat scatterings on all length scales on the same footing. The first step, decimation, consists of projecting the Green's function $G=(z-H)^{-1}$ on a subspace spanned by orbitals at alternating unit cells. The average over occupation of decimated sites is then performed using some effective-medium theory, so that the Green's function on the new length scale has the same form as on the old one. In this way, renormalization-group equations are obtained relating Green's function elements on different length scales. These equations are iterated until the fixed point is reached—where the Green's function can be simply calculated.

When the RG methods are applied to polydiacetylene it is necessary to decimate over alternating monomers, as

shown in Fig. 7(b), in order to preserve the structure of the chain on the new length scale. To average over configurations of decimated monomers, we split the Hamiltonian in the following way:

$$H=\tilde{H}+\delta H \ , \tag{3.2}$$

where δH consists of double bond hoppings:

$$\begin{aligned}\delta H&=\sum_n \delta H_n \ ,\\ \delta H_n&=V_2[\,|\,6n+6\rangle\langle 6n+7\,|\\ &\quad+|\,6n+7\rangle\langle 6n+6\,|\,]\end{aligned} \tag{3.3}$$

and $\tilde{H}$ reflects *isolated, but disordered,* monomers:

$$\begin{aligned}\tilde{H}&=\sum_n \tilde{H}_n \ ,\\ \tilde{H}_n&=\sum_{i,j=1}^{6} t_{6n+i,6n+j}\,|\,6n+i\rangle\langle 6n+j\,|\ .\end{aligned} \tag{3.4}$$

Following Ref. 32, we then consider δH as a perturbation and consider the T matrices corresponding to δH_n:

$$T_n^{(0)}=\delta H_n+\delta H_n\,\tilde{G}\,\delta H_n+\cdots=\delta H_n(1-\tilde{G}\,\delta H_n)^{-1} \ . \tag{3.5}$$

The quantity $\tilde{G}(z)=(z-\tilde{H})^{-1}$ is the "unperturbed" Green's function. Since $\tilde{H}$ is block diagonal in 6×6 matrices, $\tilde{G}$ also has this form, so that the corresponding matrix elements can be easily calculated. Note that, although δH_n does not depend on any rotational angle, $T_n^{(0)}$ does because $\tilde{G}$ itself is a function of conformation. The result for $T_n^{(0)}$ is

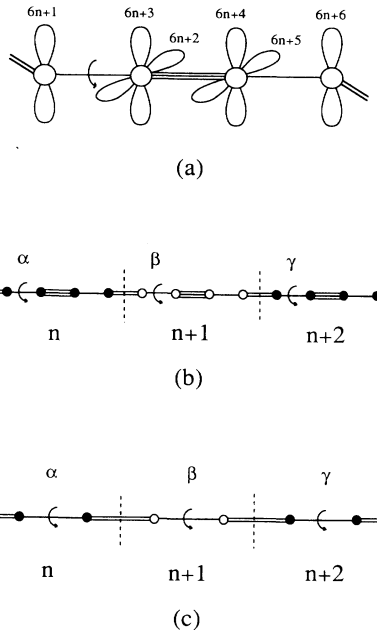

FIG. 7. Labeling of orbitals in polydiacetylene monomer n (unit cell n) is shown in (a). When the decimation is performed, the Green's function is projected onto alternating monomers, as illustrated by the blackened sites in (b); the averaging is then done over the decimated (white) sites. A simplified electronic structure model (and the appropriate decimation scheme) is displayed in (c). This latter model is used only for localization length calculations.

$$\begin{aligned}T_n^{(0)}(\alpha_n,\alpha_{n+1})&=a^{(0)}(\alpha_n,\alpha_{n+1})\,|\,6n+6\rangle\langle 6n+6\,|+b^{(0)}(\alpha_n,\alpha_{n+1})\,|\,6n+6\rangle\langle 6n+7\,|\\ &\quad+b^{(0)}(\alpha_{n+1},\alpha_n)\,|\,6n+7\rangle\langle 6n+6\,|+a^{(0)}(\alpha_{n+1},\alpha_n)\,|\,6n+7\rangle\langle 6n+7\,|\ ,\end{aligned} \tag{3.6}$$

where α stands for both the rotational angle ϕ and the hydrogen-bond-indicating variable μ, and

$$\begin{aligned}a^{(0)}(\alpha,\beta)&=V_2^2G_d(\beta)/[1-V_2^2G_d(\alpha)G_d(\beta)] \ ,\\ b^{(0)}(\alpha,\beta)&=V_2/[1-V_2^2G_d(\alpha)G_d(\beta)] \ .\end{aligned}$$

The quantity $G_d(\alpha_n)$ is a diagonal matrix element of the unperturbed Green's function

$$\begin{aligned}G_d(\alpha_n)&\equiv\langle 6n\,|\,\tilde{G}\,|\,6n\rangle=\langle 6n+6\,|\,\tilde{G}\,|\,6n+6\rangle\\ &=z(z^2-V_3^2)(z^2-V_3^2-V_1^2)\\ &\quad\times[z^2(z^2-V_1^2-V_3^2)^2-V_1^4V_3^2\cos\phi_n]^{-1} \ .\end{aligned}$$

Given the T matrices, the full Green's function can be expressed as

$$\begin{aligned}G&=\tilde{G}+\tilde{G}\left[\sum_n T_n^{(0)}\right]\tilde{G}\\ &\quad+\tilde{G}\left[\sum_n T_n^{(0)}\right]\tilde{G}\left[\sum_{m\,(\neq n)} T_m^{(0)}\right]\tilde{G}+\cdots \ .\end{aligned} \tag{3.7}$$

The decimation procedure then consists of projecting G onto alternating monomers (n even):

$$G'=P_{\text{even}}GP_{\text{even}} \ ,$$

where

$$P_{\text{even}}=\sum_n\sum_{i=1}^{6}|\,2n+i\rangle\langle 2n+i\,|$$

are the appropriate projectors. In order to cast the Green's function on the new length scale into the same form as the old one, we can write

$$G'=\tilde{G}'+\tilde{G}'\left[\sum_n T'_{2n}\right]\tilde{G}' +\tilde{G}'\left[\sum_n T'_{2n}\right]\tilde{G}'\left[\sum_{m\,(\neq n)} T'_{2m}\right]\tilde{G}' , \tag{3.8}$$

where $\tilde{G}'=P_{\text{even}}\tilde{G}P_{\text{even}}$ is the unperturbed Green's function on the new scale and T'_{2n} is the T matrix corresponding to the perturbation $\delta H'_{2n}=\delta H_{2n}+\delta H_{2n+1}$.

The approximate averaging over the conformation of decimated monomers can be performed, within RATM, by replacing the average of products of T'_{2n} matrices by products of averages, leading to the desired Green's function on the new scale

$$G^{(1)}=\langle G'\rangle_{\text{odd}}\cong\tilde{G}^{(1)}+\tilde{G}^{(1)}\left[\sum_n T^{(1)}_{2n}\right]\tilde{G}^{(1)}+\tilde{G}^{(1)}\left[\sum_n T^{(1)}_{2n}\right]\tilde{G}^{(1)}\left[\sum_{m\,(\neq n)} T^{(1)}_{2m}\right]\tilde{G}^{(1)}+\cdots \tag{3.9}$$

with $\tilde{G}^{(1)}\equiv\tilde{G}'$ and $T^{(1)}_{2n}=\langle T'_{2n}\rangle_{\text{odd}}$. Hence it is the relationship between the matrix elements of T matrices on the old and new length scales which defines the RG equations. The detailed derivations are given in the Appendix, but the final result is that

$$\begin{aligned} a^{(N+1)}(\alpha,\gamma)&=\sum_\beta P^{(N)}(\alpha,\beta,\gamma)[a^{(N)}(\alpha,\beta)+G_H^2(\beta)a^{(N)}(\beta,\gamma)b^{(N)}(\alpha,\beta)b^{(N)}(\beta,\alpha)/d^{(N)}(\alpha,\beta,\gamma)] ,\\ b^{(N+1)}(\alpha,\gamma)&=\sum_\beta P^{(N)}(\alpha,\beta,\gamma)G_H(\beta)b^{(N)}(\alpha,\beta)b^{(N)}(\beta,\gamma)/d^{(N)}(\alpha,\beta,\gamma) ,\end{aligned} \tag{3.10a}$$

with

$$\begin{aligned} d^{(N)}(\alpha,\beta,\gamma)&\equiv 1-G_H^2(\beta)a^{(N)}(\beta,\alpha)a^{(N)}(\beta,\gamma) ,\\ G_H(\beta)&\equiv\langle 6n+6\,|\,\tilde{G}\,|\,6n+1\rangle=\langle 6n+1\,|\,\tilde{G}\,|\,6n+6\rangle\\ &=-V_3V_1^2(z^2-V_3^2)\cos\phi_\beta/[z^2(z^2-V_1^2-V_3^2)^2-V_1^4V_3^2\cos^2\phi_\beta] .\end{aligned} \tag{3.10b}$$

Recall that β stands for the conformational state $\{\mu_\beta,\phi_\beta\}$, so that

$$\sum_\beta\equiv\sum_{\mu_\beta}\int_0^{\pi/2}d\phi_\beta .$$

In these equations, use is made of the probability distribution $P^{(N)}(\alpha,\beta,\gamma)$, the probability (at iteration step N) of a monomer having a conformation β if the neighboring monomers have conformations α and γ, respectively:

$$\begin{aligned} P^{(N)}(\alpha,\beta,\gamma)&=[Z^{(N)}(\alpha,\gamma)]^{-1}\exp[K^{(N)}(\mu_\alpha+\mu_\gamma)\mu_\beta+h^{(N)}\mu_\beta][(1-\mu_\beta)\delta(\phi_\beta)+(2/\pi)\mu_\beta] ,\\ Z^{(N)}(\alpha,\gamma)&=\sum_{\mu_\beta}\int_0^{\pi/2}d\phi_\beta P^{(N)}(\alpha,\beta,\gamma),\quad K^{(0)}\equiv S_{\text{ch}}/k,\quad h^{(0)}\equiv -E_b/kT .\end{aligned} \tag{3.11}$$

The reason we have to specify step N is that when the decimation is performed, this probability distribution also gets renormalized. It preserves the same form on every length scale, but the values of K and h are changed according to the RG equations

$$\begin{aligned} K^{(N+1)}&=\ln\{\cosh(K^{(N)}+\tfrac{1}{2}h^{(N)})\cosh(\tfrac{1}{2}h^{(N)})/\cosh^2[\tfrac{1}{2}(K^{(N)}+h^{(N)})]\} ,\\ h^{(N+1)}&=h^{(N)}+K^{(N)}+2\ln\{\cosh[\tfrac{1}{2}(K^{(N)}+h^{(N)})]/\cosh(\tfrac{1}{2}h^{(N)}]\} .\end{aligned} \tag{3.12}$$

These RG equations are easily derived using the standard decimation procedure for the one-dimensional Ising model.[45]

This entire set of renormalization-group equations, Eqs. (3.10)–(3.12), can be iterated until the fixed point is reached. There $b^{(\infty)}(\alpha,\beta)=0$, so the resulting T matrices are diagonal. Moreover, it is easy to see that $a^{(\infty)}(\alpha,\beta)=a^{(\infty)}(\alpha)$ (independent of β), which means that the T matrices can be regarded as corresponding to diagonal perturbations at the end sites of each monomer. At the fixed point, therefore, the system consists of disconnected monomers with an effective Hamiltonian

$$H_{\text{eff}}=\sum_j H_j^{(\infty)} , \tag{3.13}$$

where the sum is over the undecimated (remaining) monomers and

$$\begin{aligned} H_j^{(\infty)}&=\tilde{H}_j(\alpha_j)+\varepsilon'(\alpha_j)[\,|\,6j+1\rangle\langle 6j+1\,|\\ &\qquad+|\,6j+6\rangle\langle 6j+6\,|\,] ,\\ \varepsilon'(\alpha)&=a^{(\infty)}(\alpha)/[1+a^{(\infty)}(\alpha)G_d(\alpha)] .\end{aligned} \tag{3.14}$$

This result follows from the fact that a diagonal perturbation $\varepsilon'(\alpha)\,|\,\alpha\rangle\langle\alpha\,|$ has a corresponding T matrix:

$$\begin{aligned} T_a&=\{\varepsilon'(\alpha)/[1-\varepsilon'(\alpha)G_d(\alpha)]\}\,|\,\alpha\rangle\langle\alpha\,|\\ &\equiv a^{(\infty)}(\alpha)\,|\,\alpha\rangle\langle\alpha\,| .\end{aligned}$$

Since our effective Hamiltonian is block diagonal, the fixed-point Green's function $G^{(\infty)}$ can be calculated easily. The averages over conformations of remaining monomers can be performed independently, since $K^{(\infty)}=0$, so that the probability distribution is uncorrelated at the fixed point. The resulting expression for the trace of the average Green's function (per monomer) is

$$\mathrm{Tr}\langle G\rangle=\sum_{\beta}P^{(\infty)}(\beta)\mathrm{Tr}G^{(\infty)}(\beta)\ , \tag{3.15}$$

where

$$\mathrm{Tr}\,G^{(\infty)}(\beta)=(2z\{z^2+2z[z-\varepsilon'(\beta)]-V_1^2-V_3^2\}\{z[z-\varepsilon'(\beta)]-V_1^2-[z-\varepsilon'(\beta)]V_3^2/z\})$$
$$\times(z^2\{z[z-\varepsilon'(\beta)]-V_1^2-[z-\varepsilon'(\beta)]V_3^2/z\}^2-V_1^4V_3^2\cos^2\phi_\beta)^{-1}\ , \tag{3.16}$$

which is precisely what we need to obtain the density of states per monomer:

$$\rho(E)=\lim_{\eta\to 0+}[(-1/\pi)\mathrm{Im}(\mathrm{Tr}\langle G(E+i\eta)\rangle)]\ . \tag{3.17}$$

With the aid of this formula we have calculated the π electron density of states for our model of polydiacetylene. The empirical values for V_1, V_2, and V_3 quoted in Sec. II were used and the results evaluated with $\eta=0.01$ eV (defining the energy resolution) in order to make the plotting possible. We have also chosen the values of K and h referred to earlier, $S_{\mathrm{ch}}/k=6.6$ and $E_b=6.6(330\ \mathrm{K})$, so that the transition takes place at $T_c=330$ K. In Fig. 8 the density of states (DOS) per monomer is presented at $T=T_c$. By comparison with the virtual-crystal prediction, Fig. 6, we observe that a considerable amount of new structure is obtained when the nontrivial effects of disorder are included. To understand the origin of this structure we calculated the DOS for different temperatures across the transition. Figure 9 shows the DOS in the energy range which is important for optical transitions (near the optical gap).

The most striking feature of Fig. 9 is the presence of an isosbestic point, in agreement with experiment,[13] but a closer look reveals interesting facets. At low temperatures, below the transition, the DOS is similar to the one for the perfect chain, since most of the hydrogen bonds are unbroken and the rotations are unlikely. At intermediate temperatures, $T\sim T_c$, new structure appears. The peaks at 1.3—1.5 eV correspond to states localized in *coiled* parts of the chain since they persist at $T\gg T_c$ where the whole chain is essentially coiled. However, the new structure in the range 1.1—1.25 eV is present only at intermediate temperatures and thus can be interpreted as due to scattering from the *interfaces* between extended and coiled parts of the chain. This structure must therefore be caused by the additional binary disorder present at intermediate temperatures. If this idea is correct, these peaks should be very sensitive to changes in the amount of short-range order. To verify this, we calculated the DOS at $T=T_c$, but with a different value of K (short-range order). In Fig. 10 the DOS for $T=T_c$ and $K=6.6$ and 4.0 are plotted. We see that at $K=4$ (less short-range order, more binary disorder) the structure from 1.1—1.25 eV is enhanced, as expected. On the other hand, the structure from 1.3—1.5 eV is not significantly affected since it corresponds to the uncorrelated, continuous disorder which is due to rotations within coiled segments.

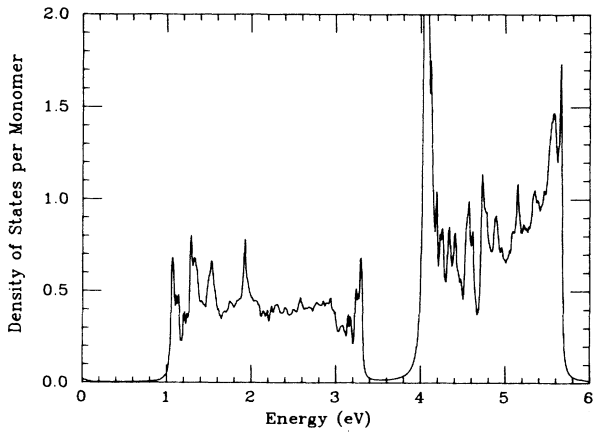

FIG. 8. Density of states calculated from RATM at $T=T_c=330$ K. The conformational disorder clearly introduces a significant amount of new structure. However, even in the presence of disorder the density of states should exhibit gaps below 1.05 eV and from 3.3 to 4.06 eV. The apparent band tails are a result of the finite energy resolution used in the calculation ($\eta=0.01$ eV). For this figure $S_{\mathrm{ch}}/k=6.6$.

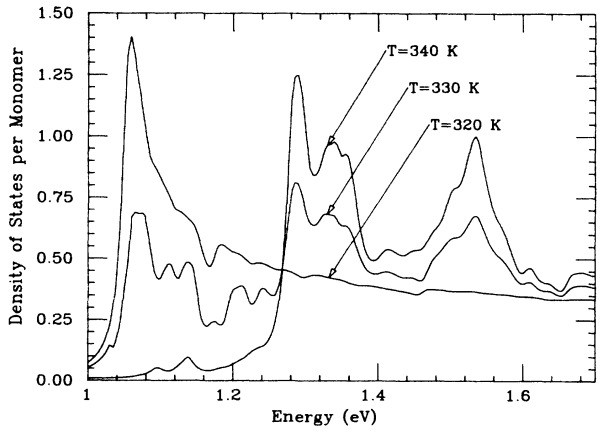

FIG. 9. RATM density of states over the optically relevant energy range for temperatures below, at, and above the conformational transition. The parameters used are the same as those in Fig. 8. Note the presence of an isobestic point at ~ 1.27 eV. and the existence of some features (such as those in the 1.1—1.25-eV range) which only exist at intermediate temperatures.

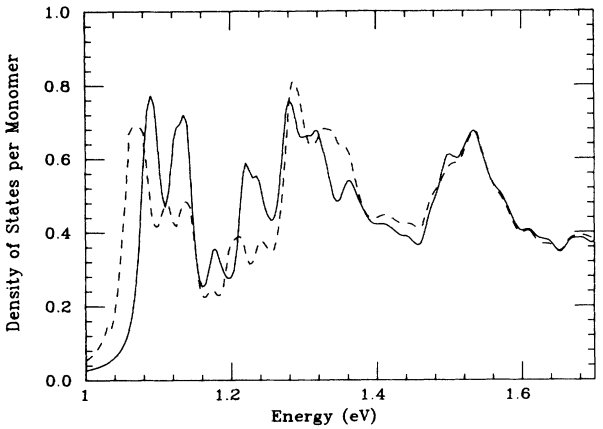

FIG. 10. Changes in the RATM density of states as the amount of short-range order is varied. The curves are for $T=T_c=330$ K with the two different values of side-chain entropy referred to in Fig. 5: the dashed curve is for $S_{ch}/k=6.6$ (as in Figs. 8 and 9) and the solid curve is for $S_{ch}/k=4.0$ (less short-range order, more binary disorder). Increasing disorder apparently enhances features in the 1.1—1.25-eV range.

C. Localization length

As we alluded to in the Introduction, there is an exact relationship between the localization length and the density of states of one-dimensional systems,[34]

$$\lambda(E)=\int \rho(\varepsilon)\ln|E-\varepsilon|\,d\varepsilon-\ln|V| \ . \tag{3.18}$$

Here λ is the inverse localization length, ρ the density of states, and V is the geometrical mean of the off-diagonal terms in the Hamiltonian. However, because of the extreme sensitivity of $\lambda(\varepsilon)$ to the local, singular structure of the DOS, conventional effective-medium theories, which give smooth, structureless spectra, cannot be used successfully in calculations of the localization length. On the other hand, RG methods such as RATM do give highly structured and singular spectra and therefore, as recently demonstrated, give results for $\lambda(\varepsilon)$ in excellent agreement with simulations.[32]

Unfortunately, the above formula has been derived for simple chains with only one orbital per site, by making explicit use of the tridiagonal form of the corresponding Hamiltonian matrix.[34] In order to be able to apply this method directly to polydiacetylene, we make a further simplification which should not significantly affect the result in the energy range of interest. Because we are interested in optical and vibrational properties, we are mostly concerned with the structure of the low-energy band (near the optical gap). Therefore we can use a simpler model for the electronic structure which will nevertheless accurately reproduce the details of this band. This model is obtained by replacing the single-triple-single unit by an effective single bond and keeping only two orbitals per monomer [Fig. 7(c)]. Again, only rotations around single bonds are allowed and the same probability distribution for disorder is used. The effective values for the single-bond and double-bond hopping elements are chosen so that the size of the gap has the correct values, both for a perfect chain and when the rotations are present: $V_1=0.88$ eV, $V_2=1.93$ eV. In this streamlined model, as with the more accurate one, the RATM can be applied to calculate the DOS. The RG equations have the same form as before, the only difference being that the "unperturbed" part of the Hamiltonian H now has a simpler form (i.e., it consists of single-bond hoppings only). Accordingly, the matrix elements of $\tilde{G}$ are now

$$G_D(\alpha)=z/[z^2-V_1^2\cos^2\phi_\alpha] \ ,$$

$$G_H(\alpha)=V_1/[z^2-V_1^2\cos^2\phi_\alpha] \ .$$

At the fixed point,

$$\mathrm{Tr}\,G^{(\infty)}=2[z-\varepsilon'(\alpha)]/\{[z-\varepsilon'(\alpha)]^2-V_1^2\cos^2\phi_\alpha\}$$

with $\varepsilon'(\alpha)$ the same as before.

The resulting structure of the low-energy band is well reproduced, although the other bands are not present. Since $\lambda(E)$ depends essentially on the *local* structure of the DOS, we expect that the results obtained from this model will be reliable in a limited energy range. We will therefore make use of Eq. (3.18) without further comment. However, in order to apply Eq. (3.18) we need the geometric mean of hopping elements, which for this case is

$$\ln|V|=\tfrac{1}{2}\ln|V_1V_2|+\langle\mu\rangle\pi^{-1}\int_0^{\pi/2}d\phi\ln|\cos\phi| \ ,$$

where $\langle\mu\rangle$ is the fraction of broken bonds. Using RATM results for the DOS, we can then do the numerical integration to obtain λ as a function of energy. In Fig. 11

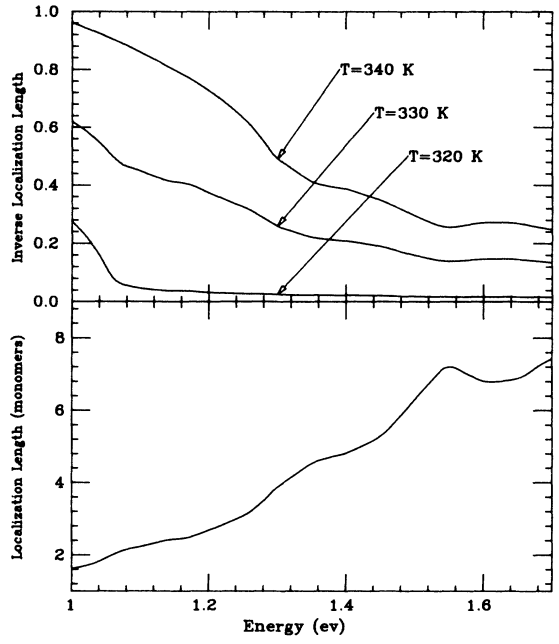

FIG. 11. Localization length λ^{-1} and inverse localization length λ (both in units of monomers) as calculated from the RATM density of states with the parameters used in Figs. 8 and 9. The top graph illustrates how the localization length decreases as temperature increases and the bottom graph (for which $T=T_c=330$ K) shows how the localization length increases as energy increases. As one can see by comparison with Fig. 9, the structure of the density of states is also reflected in the localization length: peaks and shoulders in the latter correspond to peaks in the former.

we plot λ at three different temperatures, and show the localization length itself, λ^{-1}, at $T=T_c$.

Clearly our results indicate that the localization length generally decreases with temperature, as expected, since the amount of disorder is being increased. The dependence of the localization length on energy reflects, to some extent, the structure of the DOS: Peaks in the DOS correspond to larger localization lengths (compare Figs. 9 and 11). On the average, though, the localization length increases with increasing energy—which seems paradoxical in view of the fact that higher energy features correspond to states localized in the coiled segments, where the disorder is the strongest. We suggest, in agreement with Ref. 32, that the reason for such behavior is that when correlated disorder is present, *one length scale is not enough to characterize the form of the wave functions.* States in the lower energy range, 1.0—1.3 eV, correspond to extended (rodlike) segments of the chain, as sketched in Fig. 12(a). At these energies the wave function has appreciable amplitude over length scales of order $\langle l \rangle$, the average length of extended segments (calculated in Sec. II). The localization length, on the other hand, only measures the exponential decay as one enters the coiled segments. Therefore the typical "size" of the state in this energy interval is of the order of $\langle l \rangle \gg \lambda^{-1}$. The situation is quite the opposite for the states of higher energies, 1.3—1.5 eV, corresponding to states localized in coiled segments. There, the disorder is uncorrelated and the size of the state *is* measured by the localization length [Fig. 12(b)], so that in this energy interval the typical extent of the wave function increases with energy.

IV. DISCUSSION

What we have tried to demonstrate in this paper is that conformational disorder can be an important factor in determining the electronic structure of conjugated polymers. We started with a simple model for disorder which was nonetheless sufficiently detailed to contain both uncorrelated, continuous rotations and binary disorder with strong short-range order. Our results show that such disorder, by itself, is enough to account for the existence of specific features in the density of states. Thus one does not need to invoke conformational defects with particular geometries. Moreover, the existence of disorder in conjugated polymers is therefore expected to have nontrivial effects not only on transport but also on optical and vibrational properties. We also want to emphasize the idea that two length scales are needed to characterize the form of the electronic wave functions in these systems: the localization length and the average length of the rodlike segments of the chain. Traditionally, the concept of *conjugation length* has been used to interpret a variety of specific features in experimental spectra.[6] Since the size of the optical gap decreases with the length of the conjugated region, one typically associates higher energy absorptions with shorter conjugation lengths. However, we have shown that the *localization length,* which is the only relevant length scale for uncorrelated disorder (in the coiled phase), actually increases with energy. While this result is not all that surprising, since the localization is in general stronger in the band tails,[33] it shows the inadequacy of the conjugation-length concept, especially in the high-temperature (coiled) state.[46]

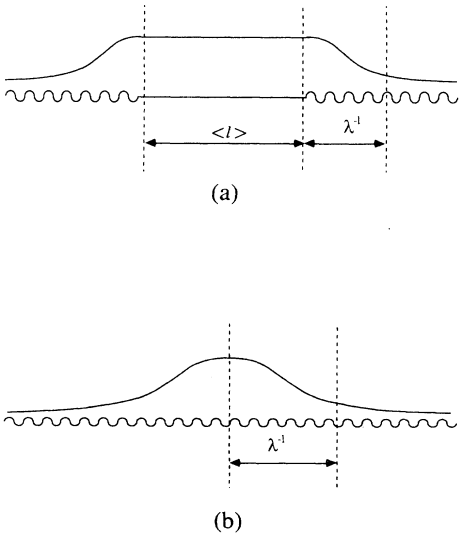

FIG. 12. Schematic representation of $|\psi|^2$ for electronic wave functions, (a) corresponding to extended segments of the polymer and (b) localized in the coiled part of the polymer. In the second situation, the localization length λ^{-1} suffices to characterize the state, but in the first an additional length scale is necessary—the average length of rodlike segments, $\langle l \rangle$.

One still has to be reasonably cautious in comparing our results directly to experiment because we have calculated only densities of states and localization lengths. To predict optical and vibrational properties one also has to calculate the appropriate transition probabilities, which themselves can be affected by disorder.[39] It would be interesting to see if the methods of this paper could be used to pursue this problem as well. Indeed, it seems likely that the same RG techniques used here could be generalized enough to permit the calculation of the average of the two-particle Green's functions needed for quantities such as the optical-absorption coefficient.

Another interesting direction for future work would be to consider the role of electron-electron correlation in presence of conformational disorder. We have already mentioned that correlations can have nontrivial effects even for perfect systems. However, upon conformational changes it is possible that such effects can become more pronounced. Even when disorder is ignored, the average value of the hopping integral (bandwidth) is reduced when the chain goes into a coiled state, and the importance of correlation is enhanced, in the Hubbard-Mott sense.[47] Furthermore, the presence of disorder itself can lead to an additional increase in the effective electron-electron interactions.[43] This behavior has been reported in other disordered systems; intuitively it follows from the fact that in presence of disorder the motion of the electrons is diffusive, so that two electrons brought together spend more time within the interaction range.[29] If this idea is correct, one can speculate on the resulting change in effective rotational potentials. We can imagine that, as some random rotations are introduced, the randomness strengthens the electronic correlations. This enhanced

correlation, in turn, decreases the effective magnitude of the (single-bond) hopping integrals and thus decreases rotational barriers. This feedback effect will allow still more randomness, possibly even driving a conformation transition in a narrow temperature range.

We should note that there is one more aspect of the behavior of polydiacetylenes in solution that has not been considered in our work, but which clearly deserves more attention. Extremely long relaxation times (days and months) have been observed[10] as the solutions are heated up through the transition and then cooled down. As demonstrated by optical and Raman measurements, the system does not return to its original low-temperature (rodlike) state. A fraction of the chain remains quenched in the coiled form in a way reminiscent of glassy behavior. Presumably, arguments about the origin of such behavior could be given within the framework of our model, in relation to the difficulty for the long and flexible side chains to realign sufficiently to remake the hydrogen bonds that stabilize the rodlike state. However, the situation is far from clear and further investigations are definitely needed in order to understand the dynamical behavior of polydiacetylenes. It is interesting to note though, that it is precisely this glassy behavior which makes possible the preparation of polydiacetylene film with different amounts of quenched-in disorder (depending on the thermal preparation of solutions from which the films are made). By performing optical and Raman measurements at low temperatures on such films, one may be able to observe the effects of disorder on the electronic structure more directly, allowing a more direct comparison with our theory.

ACKNOWLEDGMENTS

We gratefully acknowledge William M. Risen, Jr. and Jung-Mi Ha for their numerous insightful comments and for the extensive discussions we have had with them. This work was supported by the National Science Foundation (NSF) under Grant No. CHE-84-20214 and by the Brown University Materials Research Laboratory. One of us (R.M.S.) acknowledges the financial support of the Alfred P. Sloan Foundation.

APPENDIX

In this appendix we derive the relation between T-matrix elements on the old and new length scale which comprises our RG equations, Eq. (3.10). The T matrix on the new length scale is defined as

$$T'_{2n}(\alpha,\gamma)=\langle P_{\text{even}}T''_{2n}(\alpha,\beta,\gamma)P_{\text{even}}\rangle_\beta , \tag{A1}$$

where $T''_{2n}(\alpha,\beta,\gamma)$ is the T matrix corresponding to the perturbation

$$\delta H'_{2n}\equiv\delta H_{2n}+\delta H_{2n+1} . \tag{A2}$$

Accordingly, the integral equation for T''_{2n} is

$$\begin{aligned} T''_{2n}&=\delta H'_{2n}+\delta H'_{2n}\tilde{G}T''_{2n}\\ &=\delta H'_{2n}(1+\tilde{G}T''_{2n})\\ &=(\delta H_{2n}+\delta H_{2n+1})(1+\tilde{G}T''_{2n})\equiv Q_{2n}+Q_{2n+1} , \end{aligned} \tag{A3}$$

where

$$Q_i\equiv\delta H_i(1+\tilde{G}T''_{2n});\quad i=2n,2n+1 . \tag{A4}$$

We wish to express Q_i in terms of "old" T matrices. In (A4) we replace T''_{2n} by $Q_{2n}+Q_{2n+1}$ and get

$$\begin{aligned} Q_{2n}&=\delta H_{2n}[1+\tilde{G}(Q_{2n}+Q_{2n+1})] ,\\ Q_{2n+1}&=\delta H_{2n+1}[1+\tilde{G}(Q_{2n}+Q_{2n+1})] . \end{aligned} \tag{A5}$$

We can rewrite these equations as

$$\begin{aligned} Q_{2n}&=(1-\delta H_{2n}\tilde{G})^{-1}\delta H_{2n}(1+\tilde{G}Q_{n+1})\\ &\equiv T_{2n}(1+\tilde{G}Q_{2n+1}) ,\\ Q_{2n+1}&=(1-\delta H_{2n+1}\tilde{G})^{-1}\delta H_{2n}(1+\tilde{G}Q_{2n})\\ &\equiv T_{2n+1}(1+\tilde{G}Q_{2n}) . \end{aligned} \tag{A6}$$

Now, we can solve these two (matrix) equations for Q_{2n} and Q_{2n+1}:

$$\begin{aligned} Q_{2n}&=(1-T_{2n}\tilde{G}T_{2n+1}\tilde{G})^{-1}(T_{2n}+T_{2n}\tilde{G}T_{2n+1}) ,\\ Q_{2n+1}&=(1-T_{2n+1}\tilde{G}T_{2n}\tilde{G})^{-1}(T_{2n+1}+T_{2n+1}\tilde{G}\,T_{2n}) . \end{aligned} \tag{A7}$$

Since $T''_{2n}\equiv Q_{2n}+Q_{2n+1}$, we have expressed T''_{2n} in terms of T_{2n}, T_{2n+1}, and $\tilde{G}$. Using the block-diagonal form of $\tilde{G}$, and the fact that T_{2n} and T_{2n+1} are nonzero only in appropriate two-dimensional subspaces, it is now easy to calculate matrix elements of T'_{2n} in terms of elements of T_{2n}, T_{2n+1}, and $\tilde{G}$ from the above expression. The result of this lengthy but straightforward algebra are the RG equations, Eq. (3.10).

---

*Official address: Department of Physics, Brown University, Providence, RI 02912.

[1]R. E. Peierls, *Quantum Theory of Solids* (Clarendon, Oxford, 1955).

[2]W. P. Su, J. R. Schrieffer, and A. J. Heeger, Phys. Rev. B **22**, 2099 (1980), B **28**, 1138(E) (1983).

[3]J. L. Bredas, R. R. Chance, and R. Silbey, Phys. Rev. B **26**, 5843 (1982).

[4]D. Bloor, in *Quantum Chemistry of Polymers—Solid State Aspects,* edited by J. Ladik, J.-M. André, and M. Seel (D. Reidel, Dordrecht, 1984), p. 191; G. N. Patel, J. D. Witt, and Y. P. Khanna, J. Polym. Sci. Polym. Phys. Ed. **18**, 1383 (1980).

[5]See, for example, R. Hoffman, Tetrahedron **22**, 521 (1966). The energy scale for rotation is discussed in more detail in Sec. II A.

[6]G. J. Exarhos, W. M. Risen, Jr., and R. H. Baughman, J. Am. Chem. Soc. **98**, 481 (1976).

[7]Z. Iqbal, R. R. Chance, and R. H. Baughman, J. Chem. Phys. **66**, 5520 (1977).

[8]M. L. Shand, R. R. Chance, M. LePostollec, and M. Schott, Phys. Rev. B **25**, 4431 (1982).

[9]C. Plachetta, N. O. Rau, A. Hauck, and R. C. Schulz, Makro-

mol. Chem. Rapid Commun. 3, 249 (1982).
[10]J. M. Ha, R. M. Stratt, and W. M. Risen, Jr., J. Chem. Phys. 81, 2855 (1984).
[11]G. Wenz, M. A. Müller, M. Schmidt, and G. Wegner, Macromolecules 17, 837 (1984).
[12]G. N. Patel, R. R. Chance, and J. D. Witt, J. Chem. Phys. 70, 4387 (1979). BCMU is an abbreviation for butoxycarbonylmethylurethane. 3BCMU and 4BCMU are polydiacetylene systems $\leftleftharpoons RC{-}C{\equiv}C{-}CR\rightrightharpoons_n$ in which R is $-(CH_2)_3OCONHCH_2CO(C_4H_9)$ and $-(CH_2)_4OCONHCH_2CO(C_4H_9)$, respectively.
[13]K. C. Lim and A. J. Heeger, J. Chem. Phys. 82, 522 (1985).
[14]K. C. Lim, C. R. Fincher, Jr., and A. J. Heeger, Phys. Rev. Lett. 50, 1943 (1983).
[15]A. C. Plachetta and R. C. Schulz, Makromol. Chem. Rapid Commun. 3, 815 (1982).
[16]K. C. Lim, A. Kapitulnik, R. Zacher, and A. J. Heeger, J. Chem. Phys. 82, 516 (1985).
[17]Some more recent work investigating the effects of hydrogen bonding in the transition includes S. D. D. V. Rughooputh, D. Phillips, D. Bloor, and D. J. Ando, Chem. Phys. Lett. 114, 365 (1985), and also T. Kanetake, Y. Tokura, T. Koda, T. Kotaka, and H. Ohnuma, J. Phys. Soc. Jpn. 54, 4014 (1985). The presence of hydrogen-bonding side chains is apparently not a prerequisite for the color change.
[18]Von D. Kobelt and E. F. Paulus, Acta Crystallogr. Sec. B 30, 232 (1974); V. Enkelmann and J. B. Lando, *ibid.* 34, 2352 (1978); D. Day and J. Lando, J. Polym. Sci. Polym. Phys. Ed. 16, 1009 (1978).
[19]G. E. Babbitt and G. N. Patel, Macromolecules 14, 554 (1981).
[20]There has been considerable controversy as to whether the experimentally observed aggregation is, in fact, the direct cause of the color change. See Ref. 11, for example. While we tend to believe it is not, even if it were, we believe that the fundamental question would still be how changes in the polymer geometry translate into electronic structural changes. It is only this latter question which this paper considers in depth.
[21]A. Karpfen, J. Phys. C 13, 5673 (1980); Phys. Scr. T1, 79 (1982); N. A. Cade and B. Movaghar, J. Phys. C 16, 539 (1983); M. H. Whangbo, R. Hoffman, and R. B. Woodward, Proc. R. Soc. London, Ser. A 366, 23 (1979).
[22]R. M. Stratt and S. J. Smithline, J. Chem. Phys. 79, 3928 (1983).
[23]For instance, by using a tight-binding model on finite length chains, it is easy to show that both the gap size and the dimerization increase as the conjugation length is reduced.
[24]In Sec. II we perform calculations in the tight-binding model on an infinite chain with uniform rotations on single bonds, but with fixed bond lengths. We have repeated the calculation by optimizing with respect to the bond lengths and found that the dimerization increase slightly as rotations are introduced.
[25]A. J. Berlinsky, F. Wudl, K. C. Lim, C. R. Fincher, and A. J. Heeger, J. Polym. Sci. Polym. Phys. Ed. 22, 847 (1984).
[26]B. H. Zimm and J. K. Bragg, J. Chem. Phys. 31, 526 (1959); M. Ya. Azbel, Phys. Rev. B 20, 1671 (1979).
[27]N. Goldenfeld and J. W. Halley, Phys. Rev. Lett. 55, 730 (1985).
[28]K. S. Schweizer, Chem. Phys. Lett. 125, 118 (1986); J. Chem. Phys. 85, 1156 (1986); 85, 1176 (1986).
[29]P. A. Lee and T. V. Ramakrishnan, Rev. Mod. Phys. 57, 287 (1985).
[30]P. W. Anderson, Phys. Rev. 109, 1492 (1958).
[31]E. Abrahams, P. W. Anderson, D. C. Licciardello, and T. V. Ramakrishnan, Phys. Rev. Lett. 42, 673 (1979); P. W. Anderson, D. J. Thouless, E. Abrahams, and D. S. Fisher, Phys. Rev. B 22, 3519 (1980).
[32]M. O. Robbins and B. Koiller, Phys. Rev. B 27, 7703 (1983); 32, 4576 (1985).
[33]J. M. Ziman, *Models of Disorder* (Cambridge University Press, Cambridge, 1979).
[34]D. J. Thouless, J. Phys. C 5, 77 (1972).
[35]R. H. Baughman and R. R. Chance, J. Appl. Phys. 47, 4295 (1976).
[36]D. S. Boudreaux and R. R. Chance, Chem. Phys. Lett. 51, 273 (1977).
[37]If a similar analysis is repeated for rotations around double bonds, it is again found that $\pi/2$ is a maximum in energy. In this case, however, the energy scale is nearly two orders of magnitude larger: 4 eV. While this figure again is probably a gross overestimate, we can nevertheless conclude that such large rotations around double bonds should not be present at room temperatures and that it should be enough to consider rotations around single bonds only.
[38]R. J. Baxter, *Exactly Solved Models in Statistical Mechanics* (Academic, New York, 1982).
[39]E. N. Economou, *Green's Functions in Quantum Physics* (Springer-Verlag, Berlin, 1983).
[40]For an excellent review, see B. S. Hudson, B. E. Kohler, and K. Schulten, in *Excited States*, edited by E. C. Lim (Academic, New York, 1982), Vol. 6, p. 1.
[41]J. L. Brédas, M. Dory, and J. M. André, J. Chem. Phys. 83, 5242 (1985). We should nevertheless note that this reference shows that there is evidence that the low-lying transitions in polydiacetylene have an excitonic character.
[42]R. R. Chance, D. S. Boudreaux, J. L. Brédas, and R. Silbey, Phys. Rev. B 27, 1440 (1983); S. N. Dixit and S. Mazumdar, *ibid.* 29, 1824 (1984).
[43]*Electron-Electron Interactions in Disordered Systems*, edited by A. L. Efros and M. Pollak (North-Holland, Amsterdam, 1985).
[44]R. J. R. Ibañez and C. E. T. Gonçalves da Silva, Phys. Rev. B 31, 2464 (1985).
[45]D. R. Nelson and M. E. Fisher, Ann. Phys. 91, 226 (1974).
[46]Our observation that there are two distinct length scales present in this system could raise some doubts as to the validity of a renormalization-group approach—since such approaches are presumably taking advantage of an invariance to rescaling. Indeed, the practical application to critical phenomena actually relies on the invariance to rescaling being exact at the critical point in order to negate the approximations used in the rescaling. However, in the electronic structure context of this paper, one is not looking for such a critical point. Rather, the fixed point represents a situation in which the electronic structure can be done exactly and the RG transformations provide an approximate mapping from the real system to the fixed point. That being said, though, it is worth pointing out that, at its very worst (for the small-length scale properties of the system) the RG transformations are nothing but a high-level effective medium theory—which does *best* when the disorder is strongly correlated, because that is when fluctuations are a minimum. As we have noted, for the *long*-wavelength properties, such as the localization length, it is not only permissible but imperative to do some treatment at at least our (renormalized) level to allow for the multiple scattering on all length scales.
[47]N. F. Mott and E. A. Davis, *Electronic Processes in Non-Crystalline Materials* (Clarendon, Oxford, 1979), p. 104.